



Structural properties and growth evolution of diamond-like carbon films with different incident energies: A molecular dynamics study



Xiaowei Li, Peiling Ke, He Zheng, Aiying Wang*

Ningbo Key Laboratory of Marine Protection Materials, Ningbo Institute of Materials Technology and Engineering, Chinese Academy of Sciences, Ningbo 315201, PR China

ARTICLE INFO

Article history:

Received 24 November 2012
Received in revised form 1 February 2013
Accepted 23 February 2013
Available online 4 March 2013

Keywords:

Diamond-like carbon
Molecular dynamics simulation
Residual stress
Growth mechanism

ABSTRACT

Structural properties and growth evolution of diamond-like carbon (DLC) films with different incident energies were investigated systematically by the molecular dynamics simulation using a Tersoff inter-atomic potential for carbon-carbon interaction. The results revealed that the density, sp^3 fraction and residual compressive stress as a function of incident energy increased firstly and then decreased; when the incident energy was 70 eV/atom, the density could reach to 3.0 g/cm^3 with the maximal compressive stress of 15.5 GPa. Structure analysis indicated that the deviation of both bond angles and lengths from the equilibrium position led to the generation of a large residual stress, while the high compressive stress mainly attributed to the decrease of both bond angles and lengths among carbon atoms. The growth of DLC films underwent a formation process of “Line-Net” structure accompanied with the interaction of many atomic motion mechanisms, and the “Point” stage was only found for DLC films with low incident energy.

© 2013 Elsevier B.V. All rights reserved.

1. Introduction

Diamond-like carbon films (DLC) owning high hardness, low coefficient of friction, superior optical property and good chemical inertness, have been widely used as a protective coating in the industrial fields of cutting tools, molds and so on [1,2]. Especially for the good biocompatibility, DLC films are being considered as a strong candidate for the medical applications, such as heart valves [3,4], vascular stent [5] and artificial joint [6]. However, one of the most significant limitations of this coating is the high level of residual compressive stress which deteriorates the adhesive strength between the film and the substrate and leads to the failure of coated surface. Therefore, continuous efforts are being devoted to reducing residual stress and to improving physical properties of DLC films [7–12].

It is well known that the properties depend on the microscopic structure of the deposited layer. But no experimental method exists for characterizing this microstructure from the viewpoint of atomic scale. Computational simulation techniques provide a robust method for deeper insight of the microscopic structure and properties of a DLC film. Many previous works have reproduced the structure and property variations with kinetic energy of deposited carbon atoms by the molecular dynamics (MD) simulation, which

led to understand the deposition process in atomic scale [13–15]. However, the relationship of the origin and distribution of stress with structure evolution is not fully understood yet. In addition, the explanation for the growth mechanism of DLC films is still controversial. For example, the subplantation mode was generally accepted as the growth mechanism of DLC films [16,17], while Marks et al. [18] deduced a new model of energetic burial from the film deposition by MD simulation.

In the present study, the deposition of DLC films with different incident energies was carried out via MD simulation to systematically investigate the structure, properties and growth mechanism. The dependence of properties on incident energy, the origin and distribution of residual stress as well as the growth mechanism combined with the atomic motion mechanism were mainly analyzed.

2. Computational method

In order to simulate the deposition and structure of DLC films by MD simulation, the three-body empirical potential Tersoff was used to describe the interaction between the deposited carbon atoms and the diamond substrate [19]. The Tersoff potential has been proved to be an effective and accurate potential for carbon system.

Energetic atoms of C impacted on a diamond (001) single crystal substrate of $25.2210 \times 25.2210 \times 24.0758 \text{ \AA}^3$ in the x , y and z directions, which contained 2800 carbon atoms with 100 atoms per layer and was equilibrated at 300 K for 100 ps before deposition. The

* Corresponding author.

E-mail address: aywang@nimte.ac.cn (A. Wang).

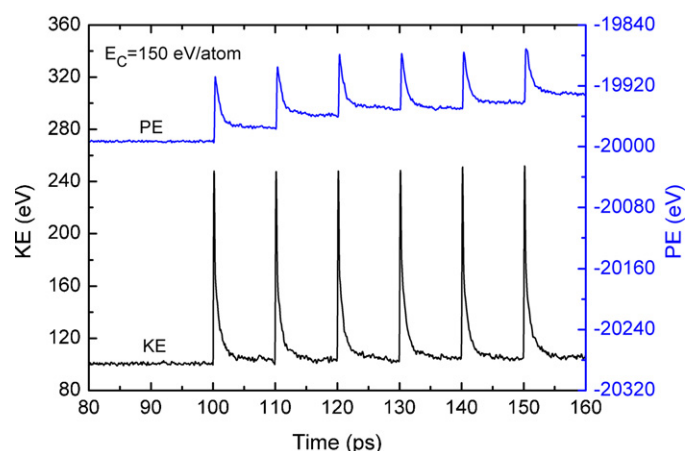


Fig. 1. Energetic variation during the deposition process when the incident energy is 150 eV/atom.

incident C atoms were deposited at the position of 10 nm above the substrate surface at a random $\{x, y\}$ position. While the positions of atoms in the bottom two layers were frozen to mimic the bulk substrate, all the other atoms were unconstrained. The incident kinetic energy of C atoms was changed from 1 eV/atom to 150 eV/atom and 2000 impacts were simulated. The periodic boundary conditions were applied in x and y directions and the time step was fixed at 1 fs.

The time interval between two sequential deposited C atoms was 10 ps, which induced an impracticable ion flux of $1.57 \times 10^{27}/\text{m}^2 \text{ s}$. Fig. 1 shows the changes in potential energy (PE)

and kinetic energy (KE) of the system during depositing the first six incident C atoms. The energy change in the system indicates that the time interval of 10 ps is enough for relaxing the atomic structure and diminishing the unrealistic effect of high carbon flux on the deposition process. The temperature of the substrate was rescaled to 300 K by the Berendsen method [20] after the atomic rearrangement caused by the bombardment of incident atom was finished. Thus it can be said that the present simulation reasonably mimic the real deposition behavior even if the simulation was under an accelerated condition.

3. Results and discussion

Fig. 2 shows the final morphologies for DLC films with the incident energies of 1 eV/atom, 70 eV/atom and 150 eV/atom, where colors represent the different coordination numbers. When the incident energy is 1 eV/atom (Fig. 2a), a film with high roughness is generated; the incident atoms have little effect on the arrangement of substrate atoms, causing an obvious interface between the film and the substrate. With increasing incident energy to 70 eV/atom, the film has a good compact structure, smaller thickness and smooth surface (Fig. 2b); because the incident energy is much higher than the cohesive energy of diamond (7.6–7.7 eV/atom), the incident atoms can implant into the diamond lattice resulting in the intermixing layer at the interface, which may induce a high stress due to impairing the regular structure of substrate. When the incident energy is 150 eV/atom, a looser structure with many defects is produced again, implying the change of mechanical properties.

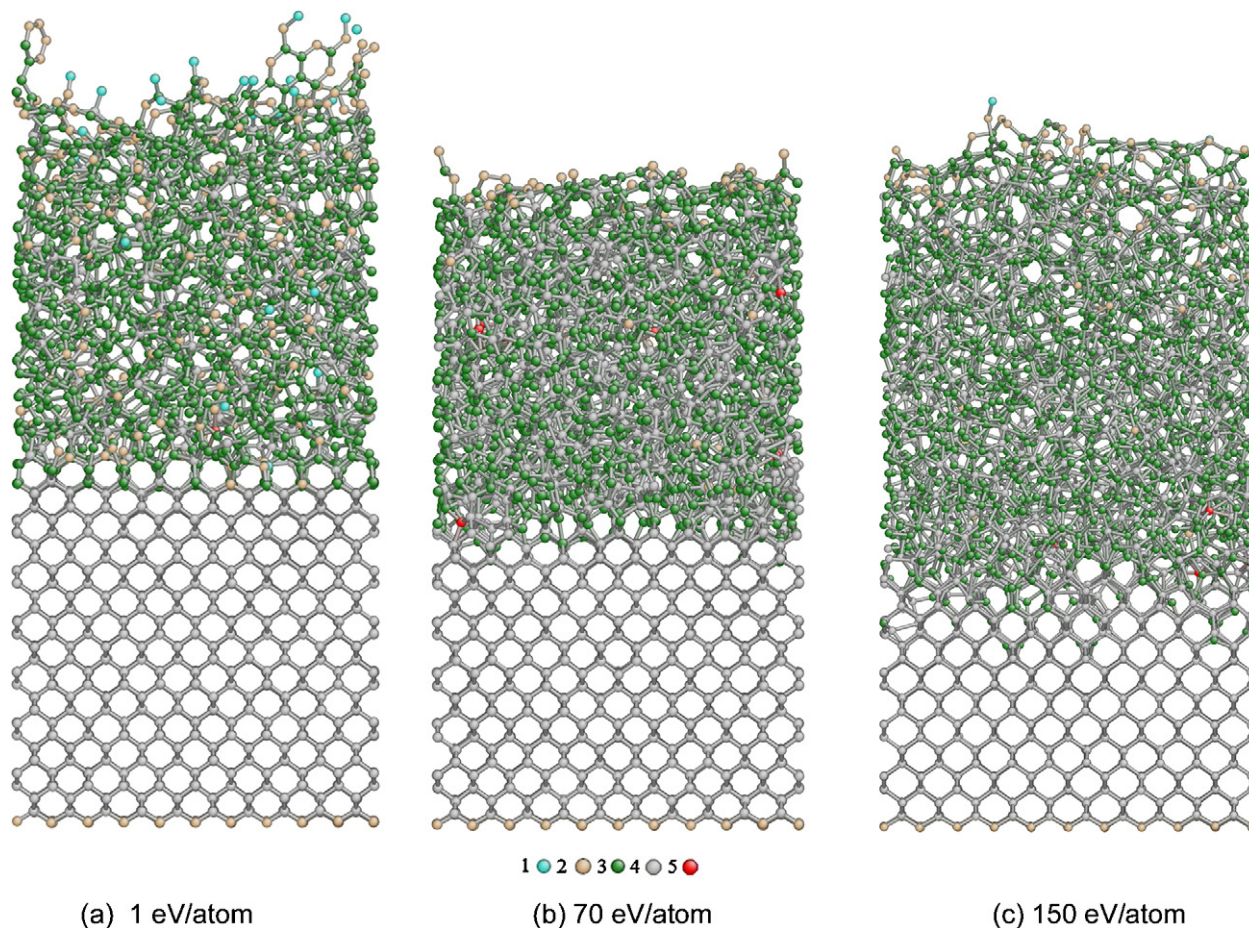


Fig. 2. Coordination configurations of films under different incident energies, where colors represent the different coordination number.

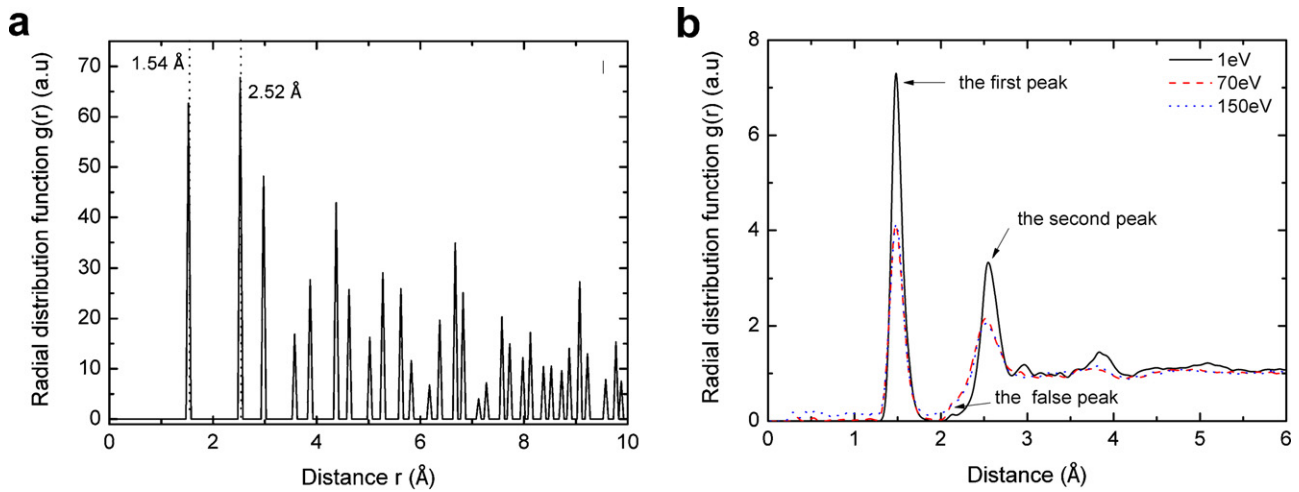


Fig. 3. RDF of (a) Diamond and (b) Films.

Taking the final configurations as objects, the radial distribution functions (RDF) of DLC films are illustrated in Fig. 3. For comparison, the RDF of crystal diamond is also included. First of all, the RDF reveals the long-range ordered arrangement of diamond (Fig. 3a), and the peaks of the first nearest neighbor and the second nearest neighbor are located at 1.52 Å and 2.54 Å, respectively. For all DLC films, the first and second peaks shown in Fig. 3b are observed at the similar positions comparing with those of diamond. This suggests the existence of similar structures between the diamond and the DLC films; besides, Fig. 3b reveals that all the films are amorphous with the characters of long-range disorder and short-range order. But except the first two amorphous peaks with narrow peak width and large peak value, other peaks toward larger interatomic distance are also observed at the energy of 1 eV/atom, implying stronger degree of order. At the position of 2.1 Å shown in Fig. 3b, the small sharp peak is caused by the cut-off radius of the Tersoff potential, termed as “false peak” [18,21].

Before charactering the dependence of films properties on incident energy, the variations of density and hybridization ratio along the film growth direction are plotted in Fig. 4 when the incident energy is 1 eV/atom or 70 eV/atom. It reveals that the whole system is divided into four regions including substrate, transition region, stable region and surface region. In the substrate region, the atomic arrangement keeps the original structure of crystal diamond and

there is no change in property. In the transition region, the amorphization comes into being gradually and the structure changes from the crystallization of diamond to the amorphization of DLC films, so the existence of structural gradient causes significant decrease in density and sp^3 fraction and increase in sp^2 fraction; with increasing the incident energy, the transition region is displaced toward the substrate direction. The surface region is also markedly relaxed, in which the variations of physical quantities drop to zero and the sp fraction has a great fluctuation. Therefore, the whole performance of the films is quantified in the stable region, where the density and hybridization ratio exhibit a relative constant value. One should note that the sp^3 fraction in all films appears low values around 15 to 33%. It might attribute to the limit of Tersoff potential where the π bonding was not adequately considered.

Fig. 5 shows the dependence of the density, residual stress and sp^3 fraction on the incident energy. The residual stress, σ , is computed by the formula

$$\sigma = \frac{P_{xx} + P_{yy} + P_{zz}}{dV} \quad (1)$$

where d is the dimensionality of the system (2 or 3 for 2d/3d), V is the system volume (or area in 2d); P_{xx} , P_{yy} and P_{zz} are the diagonal components of the stress tensor. Following the increase of incident

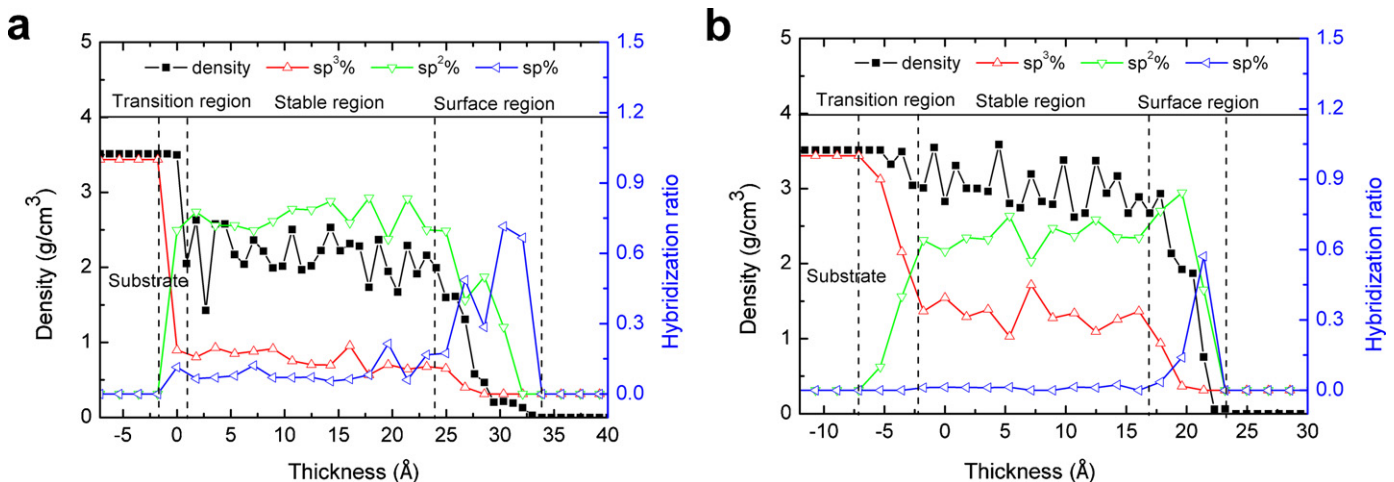


Fig. 4. Variations of density and hybridization ratio ($sp^3\%$, $sp^2\%$ or $sp\%$) along the growth direction at the incident energy of (a) 1 eV/atom and (b) 70 eV/atom. The positive direction in horizontal axis corresponds to the films, while the negative direction corresponds to the original substrate.

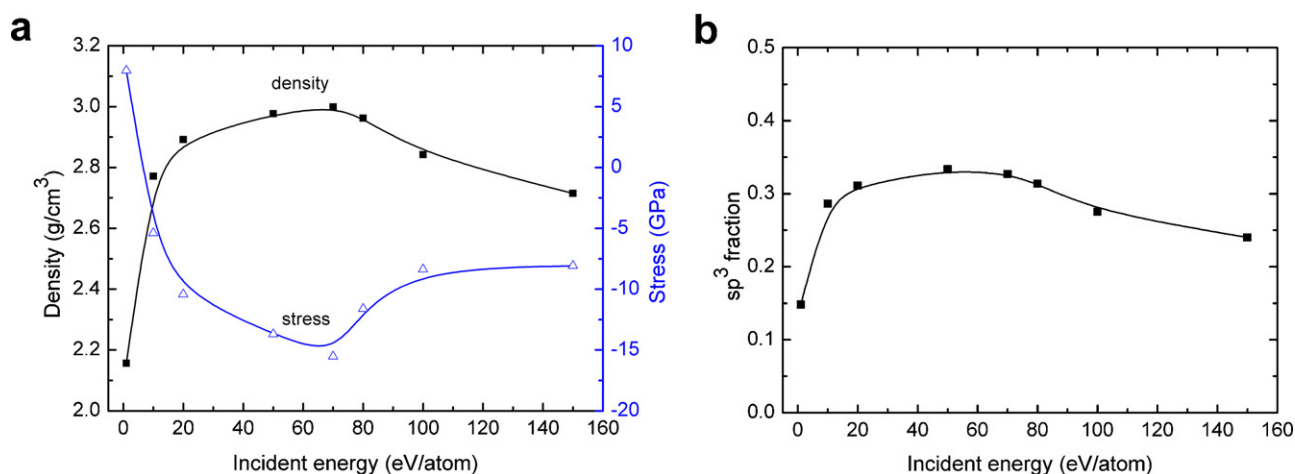


Fig. 5. Density, stress and sp^3 fraction as a function of different incident energies (a) density and stress, (b) sp^3 fraction.

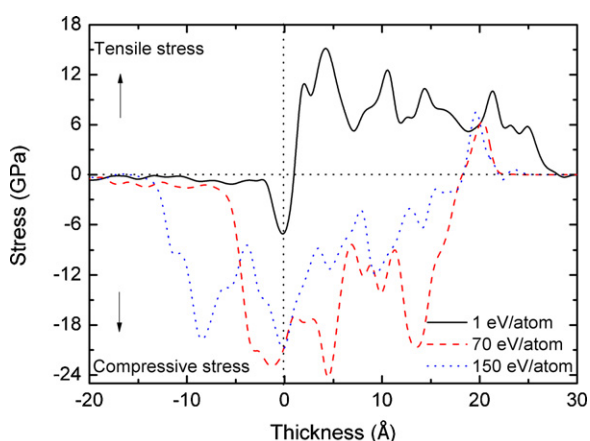


Fig. 6. Stress distribution along the growth direction under different incident energies.

energy, the density, residual compressive stress and sp^3 fraction increase rapidly and then decrease gradually. When the incident energy is 70 eV/atom, the density can reach to the maximal value of 3.0 g/cm^3 with the compressive stress of 15.5 GPa and the sp^3 fraction is 33%. In addition, Fig. 5a shows that the residual stress as a function of incident energy changes from tensile state to compressive state. The reduction of sp^3 fraction at higher incident energy

attributes to that the formed sp^3 structure is broken by high-energy deposited atoms.

The further analysis of residual stress along the growth direction is demonstrated in Fig. 6. In the case of the incident energy of 1 eV/atom, the stress state changes from the compressive stress of transition region to the tensile stress of stable region; however, the compressive stress is dominant in the DLC film with the incident energy of 70 eV/atom or 150 eV/atom. Meanwhile, the transition region shows higher stress than the stable region or the surface region for each case, which can be explained as one of the factors for the exfoliation of films.

In order to elucidate the properties in terms of the atomic bond structure variation, the bond angles and bond lengths were analyzed. Fig. 7 shows the bond angle and length distributions for DLC films at 1 eV/atom, 70 eV/atom and 150 eV/atom. It can be found that the bond angle distribution shows a peak at approximately 120° which is the graphitic bond angle, indicating that the contribution from the threefold coordinated atoms is prominent for each case. The peak value decreases and the peak width shifts toward the tetrahedral bond angle of 109.471° obviously as the incident energy increases. This is related with the increase of four-fold concentration; many distorted bond angles which are less than 109.471° are produced, resulting in the generation of high compressive stress. But at the 150 eV/atom, incident atoms can bring larger heat-affected zone, and sufficient relaxation of distorted angles is conducted, so the number of distorted angles decreases. Fig. 7b

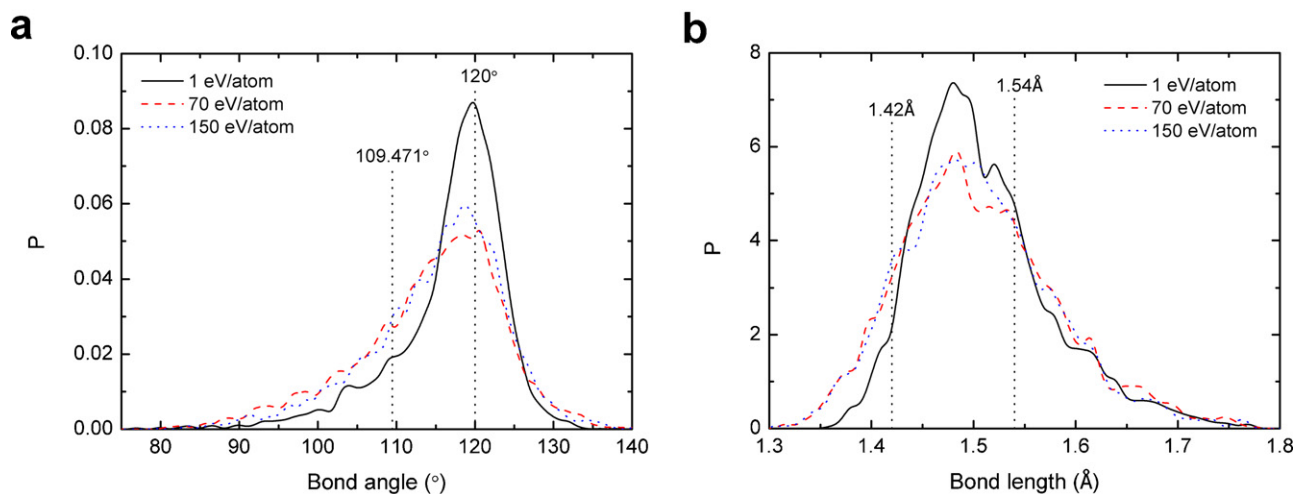


Fig. 7. Bond angle and length distribution functions (a) Bond angle distribution (b) Bond length distribution.

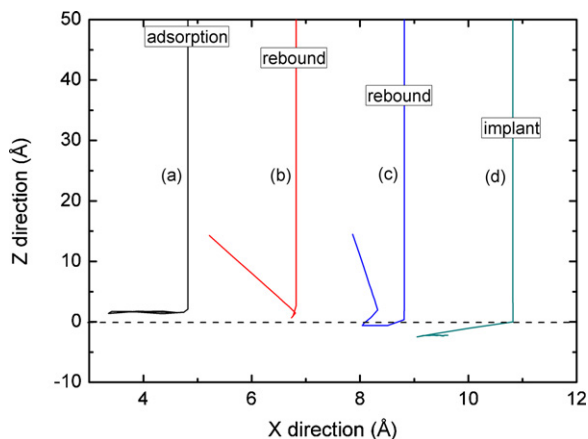


Fig. 8. Atomic motion mechanism in the deposition process of DLC films, including (a) adsorption, (b) (c) rebound and (d) implant.

reveals that the deviation of bond lengths from the equilibrium state also contributes to the residual stress. Therefore, the compressive stress mainly originates from the decrease of both bond angles and lengths among carbon atoms.

Before the growth mechanism was clarified, the motion mechanism of single incident atom with the different energies was done, which had an important effect on the structure and growth mechanism of DLC films. Fig. 8 shows the different atomic motion mechanisms in the deposition process of DLC films, including adsorption, rebound and implant.

- (1) Adsorption (Fig. 8a): it has a leading role in the range of low incident energy. The incident atoms cannot overcome the potential barrier among substrate atoms, but they can be attached to the surface and reach to an equilibrium position instantly. This mechanism is benefit for the production of sp or sp^2 hybridized structure.
- (2) Rebound (Fig. 8b, c): it can be divided into two types according to the incident energy. One is the direct rebound of atoms after interacting with surface atoms, which almost has no effect on

the films structure (Fig. 8b). The other is that deposited atoms can implant below the surface and then rebound (Fig. 8c). As for the latter, they can collide with the surrounding atoms by transferring energy and thus the formed heat-affected zone results in the relaxation and rearrangement of local atoms. It's disadvantageous to form the sp^3 bonding configuration.

- (3) Implant (Fig. 8d): atoms can be embedded into a deeper position of substrate followed by energy release to the surrounding atoms. On one hand, the existence of implant mechanism is benefit to increase density and sp^3 structure of films. On the other hand, atoms take relaxation at the same time due to the heat-affected zone, so the structure tends to be transformed from the high energetic state to the low energetic state, which brings about the decrease of density and promotes the bonding structural change from sp^3 to sp or sp^2 .

Based on the previous analysis of atomic motion mechanism, the growth of DLC films was clarified. When the incident energy is 1 eV/atom, the growth variation in initial stage is shown in Fig. 9. Because of the low energy, "adsorption" as the atomic motion mechanism takes a leading role; the deposited atoms are absorbed in the low energetic position of substrate randomly, existing in the form of "Point" (Fig. 9a). With the further deposition of carbon atoms, they joint each other to make the "Line" structure (Fig. 9b). Finally, the "Net" structure is formed by linking "Lines" (Fig. 9c), indicating the completeness of transition process from the crystalline structure to the amorphous structure. After that, the stable growth of film begins. Due to the adsorption of incident atoms, the sp^3 fraction is much lower than the sp^2 fraction (Fig. 4a) and many defects exist in this film (Fig. 2a).

When the incident energy is 70 eV/atom, deposited C atoms can implant below the substrate surface and form the "Line" structure directly, so the growth mechanism of this film only undergoes the "Line-Net" stage (Fig. 10); because partial substrate atoms obtain energy from the deposited atoms by colliding and escape from the equilibrium position, these atoms squeezed out from the substrate take part in the formation of initial structure and the ordered arrangement disappears. In all, the growth of DLC films is a dynamic process that involves the growth mode of "Point-Line-Net" and the

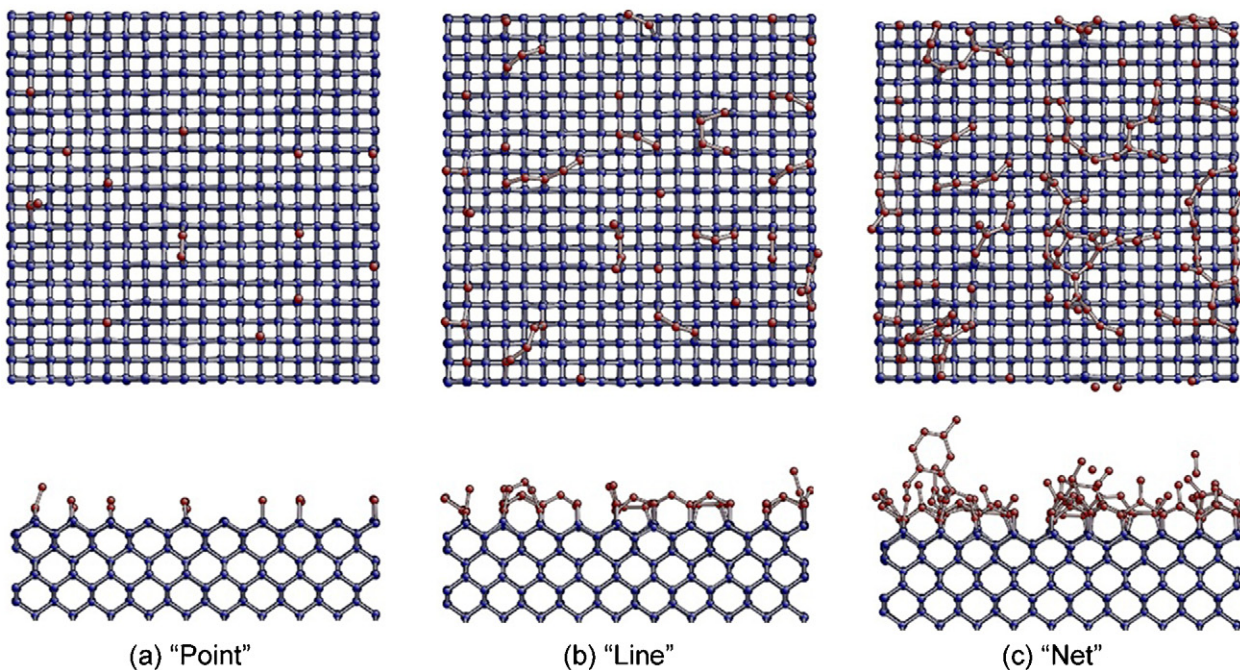


Fig. 9. Growth variation in the initial stage at the incident energy of 1 eV/atom. Blue balls represent substrate atoms and red balls represent deposited atoms.

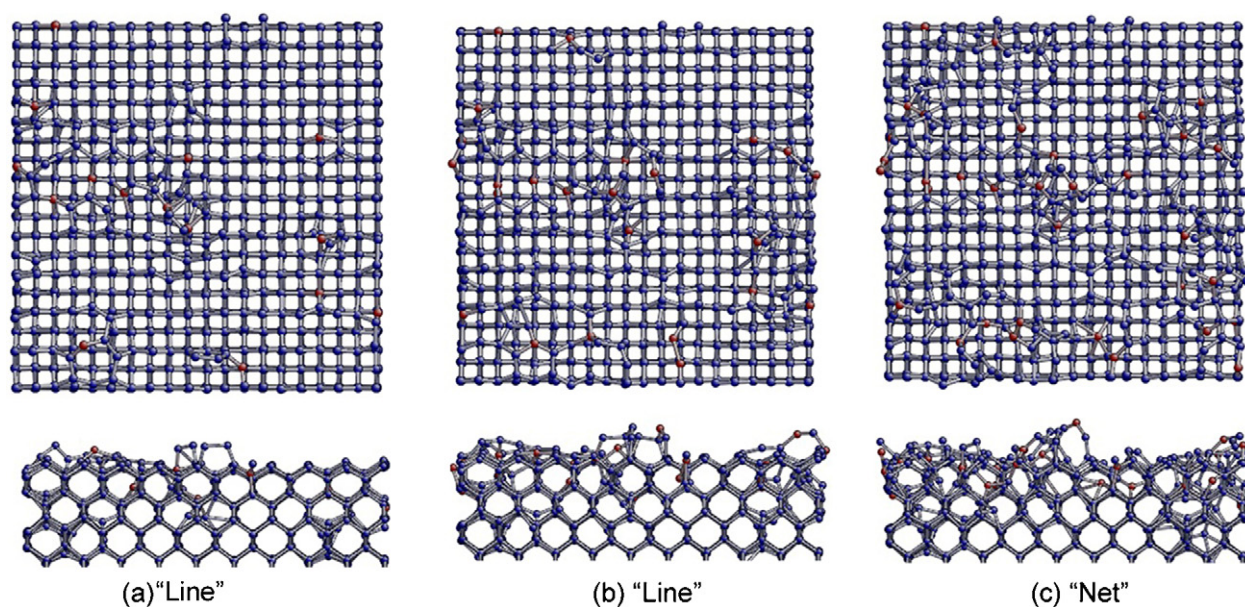


Fig. 10. Growth variation in the initial stage at the incident energy of 70 eV/atom. Blue balls represent substrate atoms and red balls represent deposited atoms.

interaction of many atomic motion mechanisms; the “Point” stage is absent at the high incident energy.

4. Conclusion

MD simulation was undertaken to investigate structural properties of DLC films with different incident energies. The Tersoff potential was used to describe the interaction between carbon atoms. The growth mechanism and atomic motion mechanism were also clarified.

With the different incident energies, the density, sp^3 fraction and compressive stress changed accordingly. When the incident energy was 70 eV/atom, the density reached to the maximal value of 3.0 g/cm^3 with the compressive stress of 15.5 GPa and the sp^3 fraction was 33%. The stress of transition region is higher than that of stable region; the analysis of both the bond angle and bond length distributions revealed that the decrease of both bond angles and lengths led to the high residual compressive stress. During the deposition process, the incident C atoms showed different motion mechanisms including adsorption, rebound and implant; the first two motion mechanisms caused a reduction of sp^3 fraction and were disadvantages to the preparation of DLC films with high quality. The DLC films were grown in the mode of “Point-Line-Net” accompanied with many atomic motion mechanisms, and there is no “Point” stage at high incident energy.

Acknowledgement

This research was supported by programs of the National Natural Science Foundation of China (51072205), and Natural Science Foundation of Zhejiang Province (Y4100156) and Ningbo Municipal Foundation (2011B1016, 2011B81001).

References

- [1] J. Brand, R. Gadow, A. Killinger, Application of diamond-like carbon coatings on steel tools in the production of precision glass components, *Surface and Coatings Technology* 180–181 (2004) 213–217.
- [2] A.H. Lettington, Applications of diamond-like carbon thin films, *Carbon* 36 (1998) 555–560.
- [3] R. Hauert, A review of modified DLC coatings for biological applications, *Diamond and Related Materials* 12 (2003) 583–589.
- [4] N. Ali, Y. Kousar, T.I. Okpalugo, V. Singh, M. Pease, A.A. Ogwu, J. Gracio, E. Titus, E.I. Meletis, M.J. Jackson, Human micro-vascular endothelial cell seeding on Cr-DLC thin films for mechanical heart valve applications, *Thin Solid Films* 515 (2006) 59–65.
- [5] P.D. Maguire, J.A. McLaughlin, T.I.T. Okpalugo, P. Lemoine, P. Papakonstantinou, E.T. McAdams, M. Needham, A.A. Ogwu, M. ball, G.A. Abbas, Mechanical stability, corrosion performance and bioresponse of amorphous diamond-like carbon for medical stents and guidewires, *Diamond and Related Materials* 14 (2005) 1277–1288.
- [6] A.S. Loir, F. garrelie, C. Donnet, J.L. Subtil, M. Belin, B. Forest, F. Rogemond, P. Laporte, Mechanical and tribological characterization of tetrahedral diamond-like carbon deposited by femtosecond pulsed laser deposition on pre-treated orthopaedic biomaterials, *Applied Surface Science* 247 (2005) 225–231.
- [7] M. Ban, T. Hasegawa, Internal stress reduction by incorporation of silicon in diamond-like carbon films, *Surface and Coatings Technology* 162 (2002) 1–5.
- [8] A.Y. Wang, K.R. Lee, J.P. Ahn, J.H. Han, Structure and mechanical properties of W incorporated diamond-like carbon films prepared by a hybrid ion beam deposition technique, *Carbon* 44 (2006) 1826–1832.
- [9] D. Sheeja, B.K. Tay, S.P. Lau, X. Shi, Tribological properties and adhesive strength of DLC coatings prepared under different substrate bias voltages, *Wear* 249 (2001) 433–439.
- [10] L.F. Bonetti, G. Capote, L.V. Santos, E.J. Corat, V.J. Trava-Airoldi, Adhesion studies of diamond-like carbon films deposited on Ti6Al4V substrate with a silicon interlayer, *Thin Solid Films* 515 (2006) 375–379.
- [11] C. Mathioudakis, P.C. Kelires, Y. Panagiotatos, P. Patsalas, C. Charitidis, S. Logothetidis, Nanomechanical properties of multilayered amorphous carbon structures, *Physical Review B* 65 (2002) 205203-1–205203-14.
- [12] W. Zhang, A. Tanaka, K. Wazumi, Y. Koga, B.S. Xu, The effect of annealing on mechanical and tribological properties of diamond-like carbon multilayer films, *Diamond and Related Materials* 13 (2004) 2166–2169.
- [13] B. Zheng, W.T. Zheng, S.S. Yu, H.W. Tian, F.L. Meng, Y.M. Wang, J.Q. Zhu, S.H. Meng, X.D. He, J.C. Han, Growth of tetrahedral amorphous carbon film: tight-binding molecular dynamics study, *Carbon* 43 (2005) 1976–1983.
- [14] E. Neyts, A. Bogaerts, R. Gijbels, J. Benedikt, M.C.M. van de Sanden, Molecular dynamics simulation for the growth of diamond-like carbon films from low kinetic energy species, *Diamond and Related Materials* 13 (2004) 1873–1881.
- [15] B.A. Pailthorpe, Molecular-dynamics simulations of atomic processes at the low-temperature diamond (1 1 1) surface, *Journal of Applied Physics* 70 (1991) 543–547.
- [16] J. Robertson, Deposition mechanisms for promoting sp^3 bonding in diamond-like carbon, *Diamond and Related Materials* 2 (1992) 984–989.
- [17] Y. Lifshitz, S.R. Kasi, J.W. Rabalais, Subplantation model for film growth from hyperthermal species: application to diamond, *Physical Review Letters* 62 (1989) 1290–1293.
- [18] N.A. Marks, Thin film deposition of tetrahedral amorphous carbon: a molecular dynamics study, *Diamond and Related Materials* 14 (2005) 1223–1231.
- [19] J. Tersoff, Empirical interatomic potential for carbon, with application to amorphous carbon, *Physical Review Letters* 61 (1988) 2879–2882.
- [20] H.J.C. Berendsen, J.P.M. Postma, W.F. van Gunsteren, A. DiNola, J.R. Haak, Molecular dynamics with coupling to an external bath, *Journal of Chemical Physics* 81 (1984) 3684–3690.
- [21] T.B. Ma, Y.Z. Hu, H. Wang, Molecular dynamics simulation of the growth and structural properties of ultra-thin diamond-like carbon films, *Acta Physica Sinica* 55 (2006) 2922–2927.